

# Tilt Angle of the Magnetic-Field Axis of Sunspots from Microwave Observations: Method and Measurement Results

N. A. Topchilo<sup>a,\*</sup> and N. G. Peterova<sup>b,\*\*</sup>

<sup>a</sup>*St. Petersburg State University, St. Petersburg, Russia*

<sup>b</sup>*Special Astrophysical Observatory, Russian Academy of Sciences, St. Petersburg, Russia*

\**e-mail: topchilona@yandex.ru*

\*\**e-mail: peterova@yandex.ru*

Received February 29, 2020; revised March 29, 2020; accepted April 29, 2020

**Abstract**—The results of the measurements of the tilt of the magnetic-field axis of sunspots for active regions (ARs) with different morphological structures are presented. The observations are taken from the data archives of the RATAN-600 radio telescope and the Nobeyama Radioheliograph (NoRH) and processed with a new measurement method proposed by us earlier (Topchilo and Peterova, 2018). The method is based on the analysis of features of the microwave cyclotron source image above the sunspot and its dynamics with respect to the angle of view when the heliographic longitude of the sunspot changes due to the Sun's rotation. We tested ten cases of observations and showed that the axis in most of them (~90%) is tilted toward the eastern limb and that the angle does not depend on the AR morphology. The degree of the tilt of the magnetic field axis of sunspots at the height of the lower part of the chromosphere–corona transition region (the boundary between them is at the height of ~2000 km) is ~1°–10° and increases with an increase in the height of the radiation source above the photosphere. Deviations from this rule are interpreted as the influence of neighboring ARs, as a result of which part of the magnetic flux of the main sunspot is closed, not on the tail of the AR as is the usual case, but on the neighboring, leading AR.

DOI: 10.1134/S0016793220070257

## 1. INTRODUCTION

Analysis of the earliest observations of the magnetic field of sunspots (SSMF), which were made at the beginning of the 20th century (Maunder, 1907), raised the question of the possible existence of deviations of the magnetic-field (MF) axis from its vertical position with respect to the photospheric surface. Measurements of the SSMF tilt were based primarily on observations in the optical band of electromagnetic radiation. They are still being carried out today with both ground-based and satellite observations. It was established (Gopasyuk, 2003, 2017; Zagainova et al., 2017) that there is some contradiction between them, not only in the magnitude of the angle but also in the tilt direction. In general, except for the contradiction, the observational material (number of measurements) remains insufficient, i.e., there are only a few cases (of the ten).

In the radio band, one can find indications that the results of sunspot observations can be interpreted based on the assumed tilt of the MF axis (Bogod and Yasnov, 2008, 2016; Vourlidis et al., 2006). Both articles use measurements of the **coordinates of cyclotron microwave-radiation sources** (CMRSs) above them. In contrast to these articles, we propose a new method for the measurement of the MF tilt-angle (MFTA) of the

sunspot based on the measurement of the **brightness temperature** of the CMRS. It is based on a distinctive feature of the mechanism of cyclotron radiation, i.e., a strong suppression of the radiation along the MF direction (Zlotnik, 1968a, 1968b) that results in the formation of a transparency window in the emitting gyro level, the parameters of which depend on the magnitude and direction of the MF, wavelength, and radiation mode. Moreover, as the wavelength decreases, the transparency window increases, and the transparency angle for the ordinary mode (o-mode) is much wider than that for the extraordinary mode (e-mode), which can be seen in observations. The proposed method of MFTA measurement consists of the analysis of the features of CMRS image dynamics over the sunspot with respect to the angle of view when the heliographic longitude of the sunspot changes due to the Sun's rotation. For an “ideal” (stable, single, and regular) sunspot, these changes must be symmetrical with respect to the time of the sunspot's passage through the central meridian (PCM) of the Sun with the minimum CMRS brightness of at the time of the PCM. However, according to microwave observations (Topchilo and Peterova, 2018, 2019), we noticed a regular advance or delay of the minimum moment with respect to the PCM moment for the geometric center

of the sunspot, which was explained by the tilt of the MF axis toward the photosphere surface.

This article describes the features of the method and the results of its application to measure the MFTA of sunspots from observations of several active regions (ARs) with different morphological structures.

## 2. DESCRIPTION OF THE METHOD AND ITS IMPLEMENTATION

One of the main observation requirements to implement the method we propose is their regularity, which should ensure the ability to measure the characteristics of the sunspot in a wide range of longitudes (ideally, from sunrise to sunset), as well as the ability to select the most suitable observational material in terms of both its quality and the sunspot morphology. There are currently two radio-band instruments that provide daily observations of the Sun, the NoRH (1.76 cm maps of the Sun, <https://solar.nro.nao.ac.jp/norh/images/>) and the RATAN-600 radio telescope (1D scans in the range (1.65–10) cm, <http://www.spbf.sao.ru/prognoz/>). We used observations from these instruments. The easiest technique of CMRS image analysis (in terms of processing) for NoRH observations is to measure the maximum brightness temperature ( $T_b$ ) on a source map (Bakunina et al., 2008). For the RATAN-600, it is more convenient to measure the excess of the maximum antenna temperature ( $T_a$ ) of the source over the background level. Figure 1 shows a sample of the used observational material, i.e., RATAN scans and NoRH maps with AR 11899 as an example, the leading sunspot of which was the closest to the concept of the ideal sunspot. A sharp change in the image can be seen due to the influence of the angle of view: the eastern edge of the source is brighter before the PCM and the western edge is brighter after the PCM. It should be noted that there is an image with a dip in its center (two-peak) close to the PCM; it is most evident in the short-wave part of the spectrum. The transition does not occur exactly at the time of the PCM but with some delay, and the delay in e-mode was greater. At the same time, there is a decrease in the maximum radio brightness and its subsequent recovery.

The SDO/HMI photoheliograms for the NOAA 11899 shown in Fig. 1 were taken during observations with the RATAN-600 (at culmination, ~0900 UT). NoRH maps were taken for the local culmination (~0244 UT) and were corrected for the time difference from the RATAN-600. For comparison with the RATAN-600, the maps were also rotated by the parallax angle of the Sun.

The temporal-temperature dynamics can be analyzed in different ways, and Fig. 2 shows some of their features. In the first variant, the difference between the minimum temperature time (MTT) and the PCM time for the geometric center of the sunspot is measured during processing. The mismatch between the

MTT and the PCM time (vertical arrows) can be clearly seen in the temperature–time graphs (bottom row of Fig. 2). The MTT–PCM time difference is converted to the sunspot MFTA according to the standard formula of the differential rotation of the Sun. This method is logically simple but inconvenient to implement, because it requires approximation of a function of an unknown type near the minimum with a 1-day interval between observations (i.e., with a rotation of ~13°).

The second variant is more interesting. It is based on the analysis of the temperature dependence on the sunspot shift relative to the center of the Sun ( $\theta$ ) (upper row of Fig. 2). Since the sunspot first approaches the center of the Sun's disk and then moves away from it, the graph of readings sorted by the time and position of the sunspot will consist of two branches, i.e., east/ascending and west/descending. For the ideal sunspot with a vertical MF, the temperature will depend only on  $\theta$ , and both branches will match regardless of their shape. For a nonzero MF tilt, the curves will split in different directions along the abscissa axis at the same distance and form a configuration similar to the hysteresis phenomenon. The distance between the branches along the abscissa axis is equal to twice the MFTA and is easily calculated. For the example shown in Fig. 2, the tilt angle is 10° in the e-mode and 3.7° in the o-mode with an accuracy of ~1°.

It should be noted only the part of the tilt angle that changes as the source moves, i.e., the angle in the direction of the Sun's rotation, is detected in the proposed variants, not the full tilt angle.

Figure 3 (right) shows the results of MFTA measurement by the above described processing methods on both instruments with the ideal leading sunspot of the NOAA 11899 group. The diamond marks the point obtained by the RATAN-600 for the 2.91-cm wave (left side of Fig. 3). The CMRS image was symmetrical at the time of the scan registration, which can be interpreted for the sunspot as an observation along the MF axis. It can be seen that all of the results for the considered case are quite consistent with each other and show an increase in tilt with wavelength, i.e., with the CMRS height above the photosphere, which we noted earlier (Topchilo and Peterova, 2018). Note that this conclusion is qualitative, and the proposed method determines the dependence of the MFTA on height by the MF model, which determines the position of gyro levels corresponding to this wavelength. However, the relative accuracy of the method can be estimated, and it will increase if the interval between observations is reduced.

The considered method was originally developed by us (Topchilo and Peterova, 2018) for an ideal sunspot, which is relatively rare. In this article, we studied the applicability of the new technique to sunspots with a more complex morphological structure and dynamics. The observational material selected from

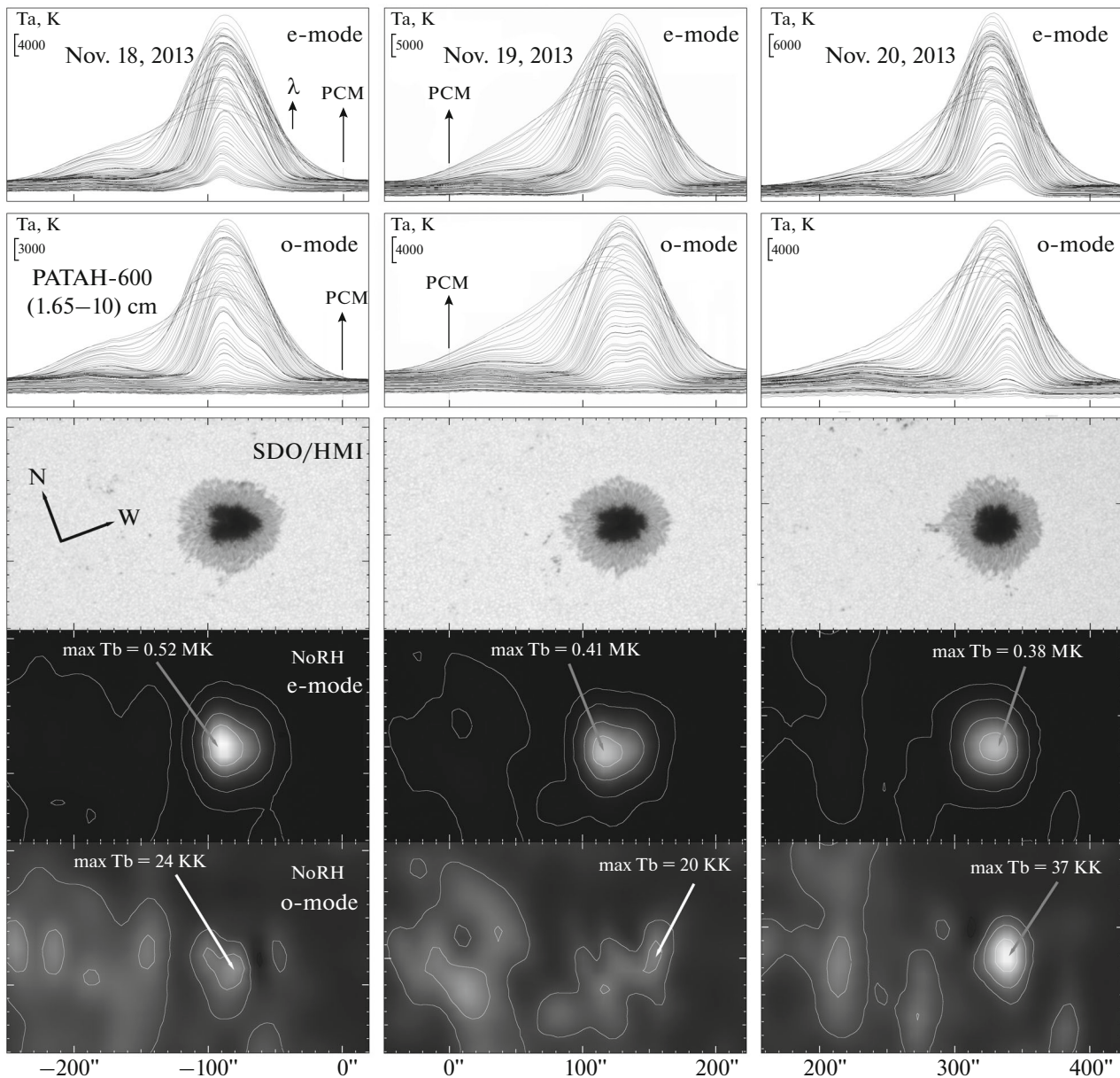


**Fig. 1.** Scans and maps of NOAA 11899 in the 1.65–10-cm range for three days, November 18–20, 2013, close to the time of passage of the center of the Sun's disk through the instrument beam (PCM), separately in e- and o-modes, according to observations by the RATAN-600 and NoRH. The direction of the wavelength increase ( $\lambda$ ) is shown in the scans. The RATAN-600 scans are presented in the antenna temperature scale (Ta), and the NoRH maps are given in the brightness temperature (Tb). Isotherms on e-mode maps: 15 KK, 40 KK, 150 KK, and 300 KK. Isotherms on o-mode maps: 15 KK, 20 KK, and 30 KK.

the RATAN-600 and NoRH archives was classified, and three types of sunspots were identified (see the examples in Fig. 4): type I includes regular, round, single, stationary sunspots; type II includes semiregular, stationary sunspots of irregular, fragmented shape; and type-III sunspots are irregular, nonstationary, and usually fragmented with an active MF. For sunspots of types I and II, the proposed technique makes it possible to estimate rather accurately the MF tilt value corresponding to the measurement results in optics (Gopasyuk, 2003, 2017). For type-III sunspots, it is

necessary to develop additional methods of MF estimation, especially for rapid sunspot evolution.

As follows from our measurement results, the sunspot MFs in most cases are tilted eastward, which fully corresponds to the established idea of the MF model in the form of a loop connecting the leading sunspot to the diffuse tail part of the AR. The conclusion is also confirmed by the fact that the tilt angle in e-mode is greater than the tilt angle in o-mode, which is generated below.

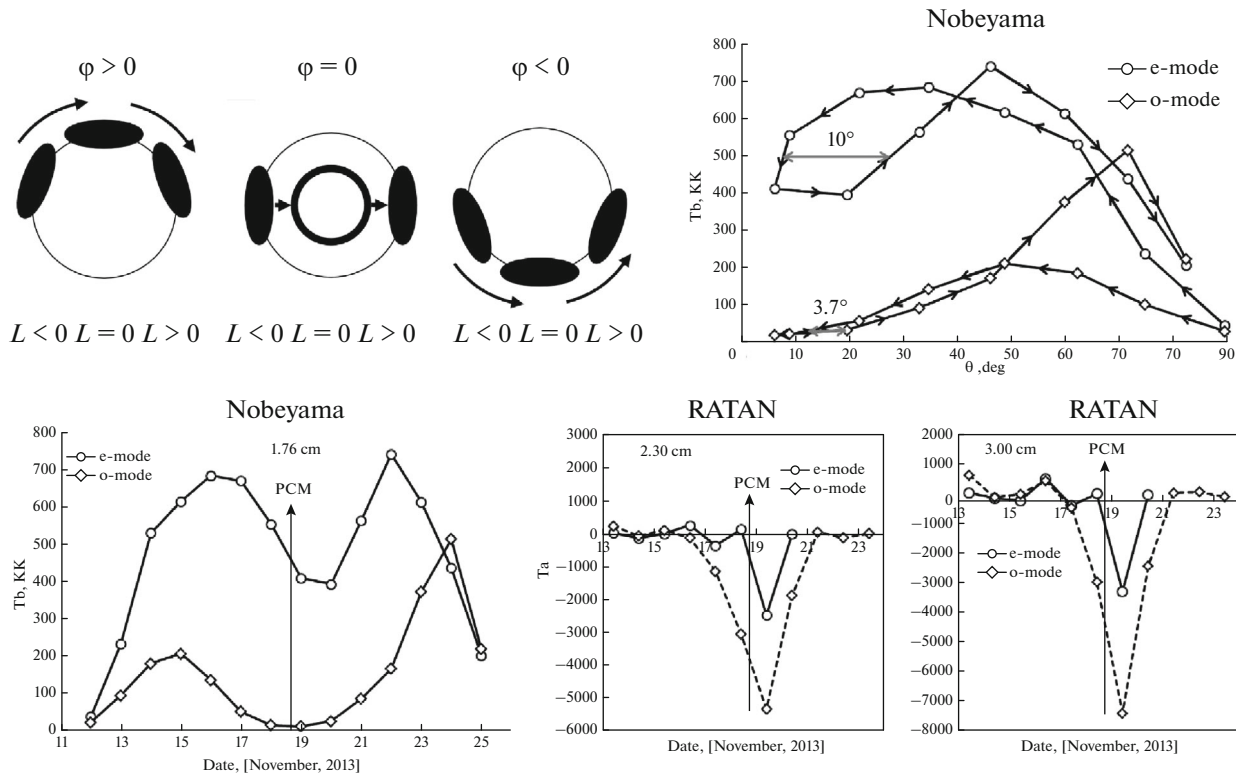


**Fig 2.** Illustration of the new technique for MF tilt measurement and its application with observations of the leading sunspot of AR 11899 (November 2013) by the RATAN-600 and Nobeyama as an example. The upper row (left) is a schematic representation of changes in the CMRS (only maximum brightness) and its position relative to the sunspot center, which is associated with an increase in the sunspot longitude ( $L$ ) for sunspots with different latitudes ( $\varphi$ ). The longitude  $L$  is measured from the central meridian. The arrows show the direction of the CMRS shift. At the top right is the observed dynamics of the brightness temperature  $T_b$  depending on the sunspot position. The arrows show how it changed over time. The bottom row shows the changes in  $T_b$  and  $T_a$  depending on time.

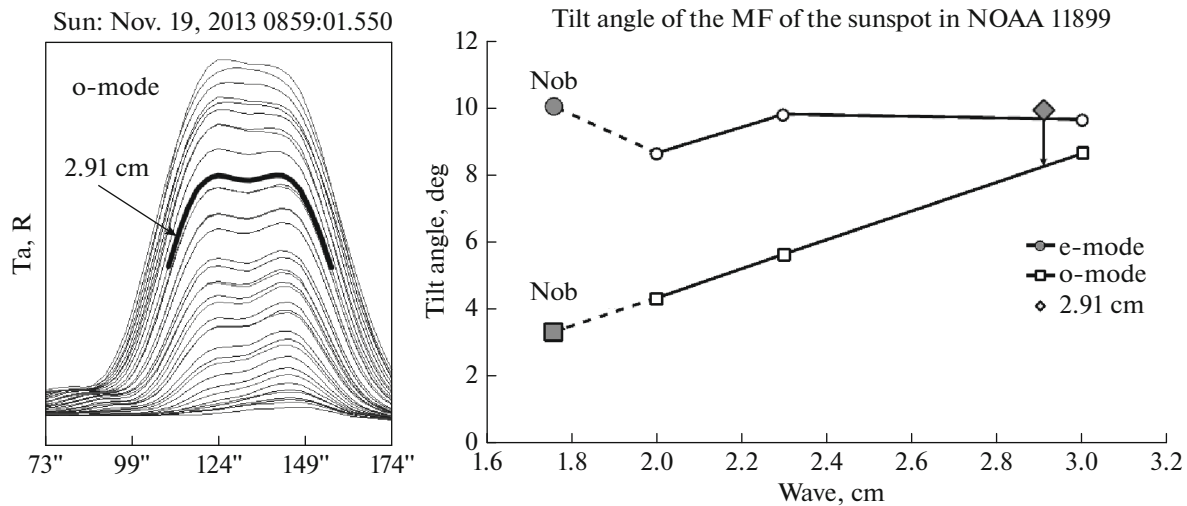


**Fig. 3.** RATAN scans of the CMRS over the leading sunspot of AR 11899 (left) and the dependence of the MFTA on the wavelength according to the data from the RATAN-600 and NoRH. The arrow indicates that the diamond belongs to measurements in o-mode.

The case of AR 11944 is almost the only deviation from this rule; Figure 5 shows the results of its observation: the tilt angle to the west is  $2.5^\circ$ – $3.5^\circ$  in o-mode and  $3^\circ$ – $5^\circ$  in e-mode.

Measurements show that the MF of the main sunspot of AR 11944 is oriented to the west (the sunspot image conversion occurred before the PCM time), and the difference in the tilt value in e- and o-modes

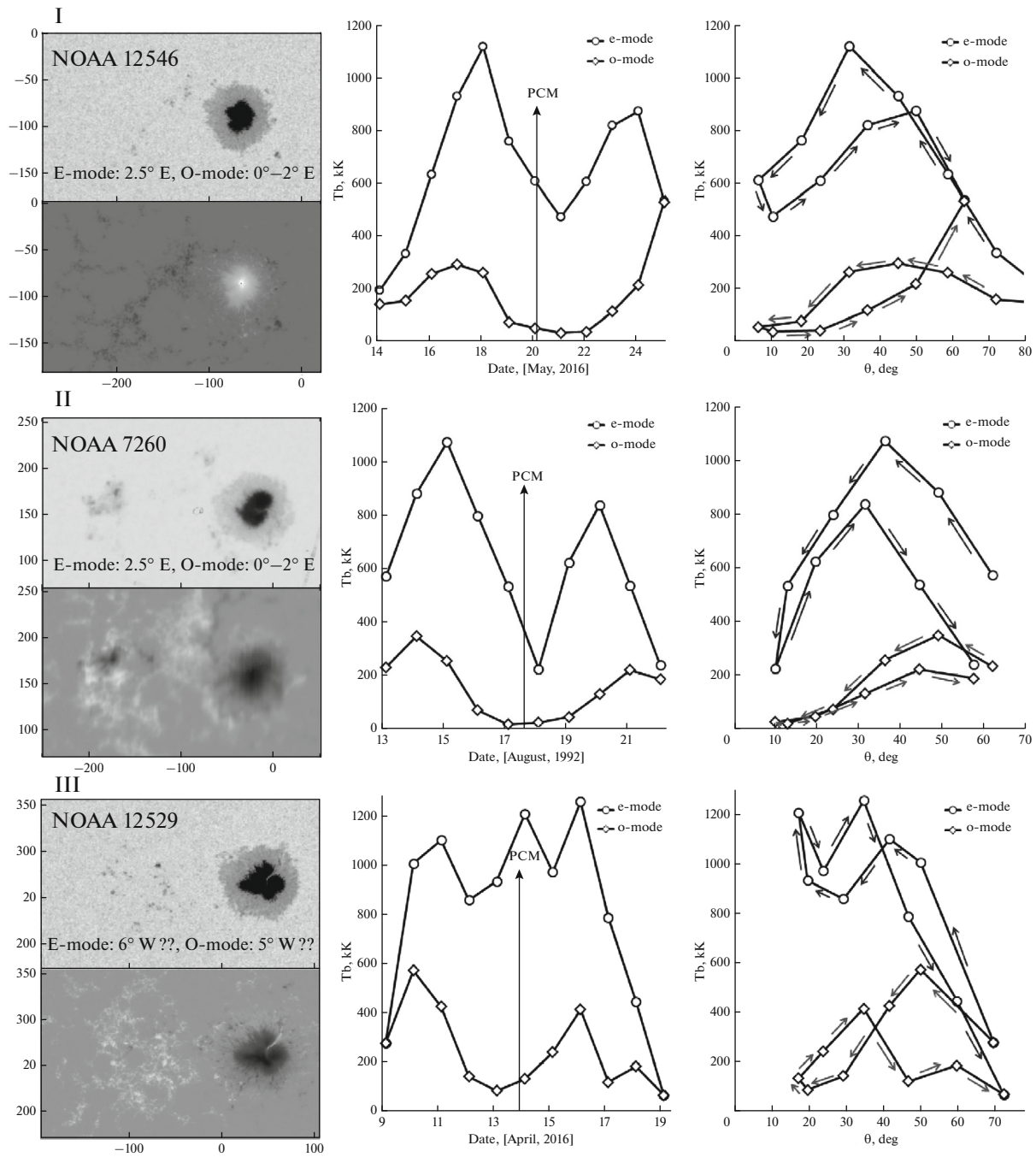


**Fig. 4.** Examples of observations of sunspots of different types (I, II, III). Left: Photoheliograms and longitudinal MF maps for the PCM moment of the sunspot. Estimates of the angle and direction of the tilt of the MF for e- and o-modes of the CMRS are also given. Right: Dynamics of brightness temperature  $T_b$  as observed by the NoRH.

is small. Examination of the magnetogram and the AR image in lines  $304 \text{ \AA}$  and  $174 \text{ \AA}$  (Fig. 6) suggests that the magnetic flux of the sunspot (N polarity) is not so much confined to the tail of its AR as to the region of opposite (S) polarity ahead of the NOAA 11943 group, which is located to the southwest of NOAA 11944. This assumption is supported by the fact that the shadow of the studied sunspot is fragmented. As a result, the

averaged MF appears to be slightly tilted (the detected tilt angle is small) to the west, and the main tilt travels the north–south line. It should be noted that, according to the RATAN-600 data, only the shortest waves in NOAA 11944 show a westward tilt of the sunspot, while longer waves as usual, demonstrate an eastward tilt.

In general, the presented results of MFTA measurements of sunspots from microwave observations

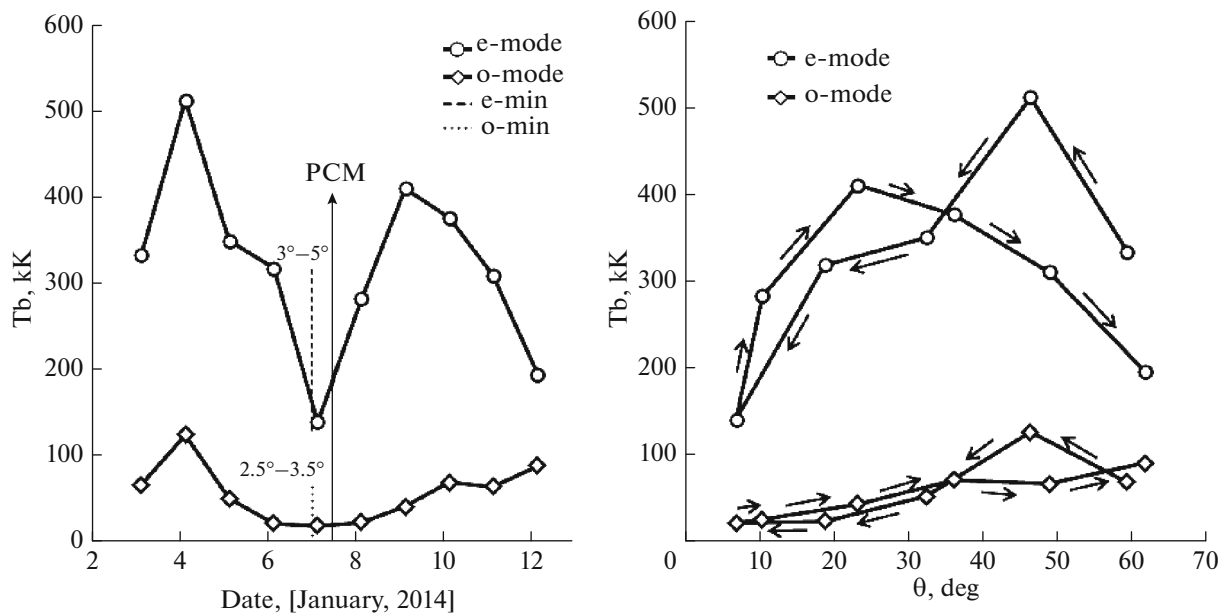


Fig. 5. Example of a nonstandard MF tilt of the sunspot in NOAA 11944 as measured by the NoRH at a wavelength of 1.76 cm.

(about ten cases) show that it is not large ( $1^\circ-10^\circ$ ) and does not depend on the AR morphology. In this case, the MF tilt is mainly directed toward the eastern limb of the Sun, as could be expected for leading sunspots, the MFs of which usually close on the tail of the AR. It was also established that the tilt angle of the sunspot MF increases with increasing wavelength (and consequently height). Basically, the changes in the tilt angle with height according to spectral observations on microwaves can be further traced throughout the chromosphere–corona transition region from 2000 km up to heights of  $\sim 10000$  km. The presented values of the tilt angles measured from observations at a wavelength of  $\sim 2$  cm are from the lower part of the transition region.

Summarizing the results of the study of our proposed method for the measurement of sunspot MFTAs, it should be noted that its application requires a stable sunspot source, especially during the passage of the central part of the disk ( $\pm 2$  days relative to the central meridian), as well as a symmetrical sunspot shape. In addition, additional research on the practical applicability of the technique for MFTA measurements of high-latitude or small sunspots is required.

### 3. DISCUSSION

The advantages of the radio band in research on the corona over sunspots are well known. In particular, tomography of the chromosphere–corona transition region is widely used on microwaves. Observations by the RATAN-600, the frequency resolution of which is now 1%, can be used to study the distribution of physical parameters of plasma with height in the corona ( $h$ ) at a resolution of  $\Delta h \sim 100$  km. Such a possible range

is provided for sources above the sunspots with cyclotron radiation, but the features of this mechanism simultaneously limit these possibilities. The CMRS image is highly dependent on the angle of view on it. The radiation maximum shifts, and its effect is summed up by the effect of the height of the source. It is impossible to separate them during observations; this can only be done via simulation (Bogod and Yasnov, 2008). Other authors (Hildebrandt et al., 1984) warned about the danger of interpreting the fine structure of the CMRS image as the result of the distribution of plasma physical parameters  $T_e$  and  $N_e$ , especially with the use of CMRS observations close to the PCM time. The angle of view also strongly influences the estimation of the CMRS height over the photosphere with the use of coordinate measurements, the accuracy of which in the radio band is limited by insufficient angular resolution. At present, it can be stated that the results of observations in the optical and radio bands are quite consistent with each other. According to Gopasyuk (2017), the tilt angle of the MF axis of sunspots is within ( $3^\circ-30^\circ$ ). Observations in the radio band do not contradict this estimate; according to Bogod and Yasnov (2008), the MF tilt is  $\sim 16^\circ$ , and we estimate it to be slightly lower ( $< 10^\circ$ ). However, these are averages. In practice, even small inaccuracies in MFTA values cause significant errors in the simulation of the CMRS of specific objects due to the features of cyclotron radiation. Therefore, a simple and fast means of its estimation is required. The advantage of the measurement method proposed by us is that it does not require cumbersome processing of the observational material, unlike the methods used in the optical and radio bands (Bogod and Yasnov, 2008). It is

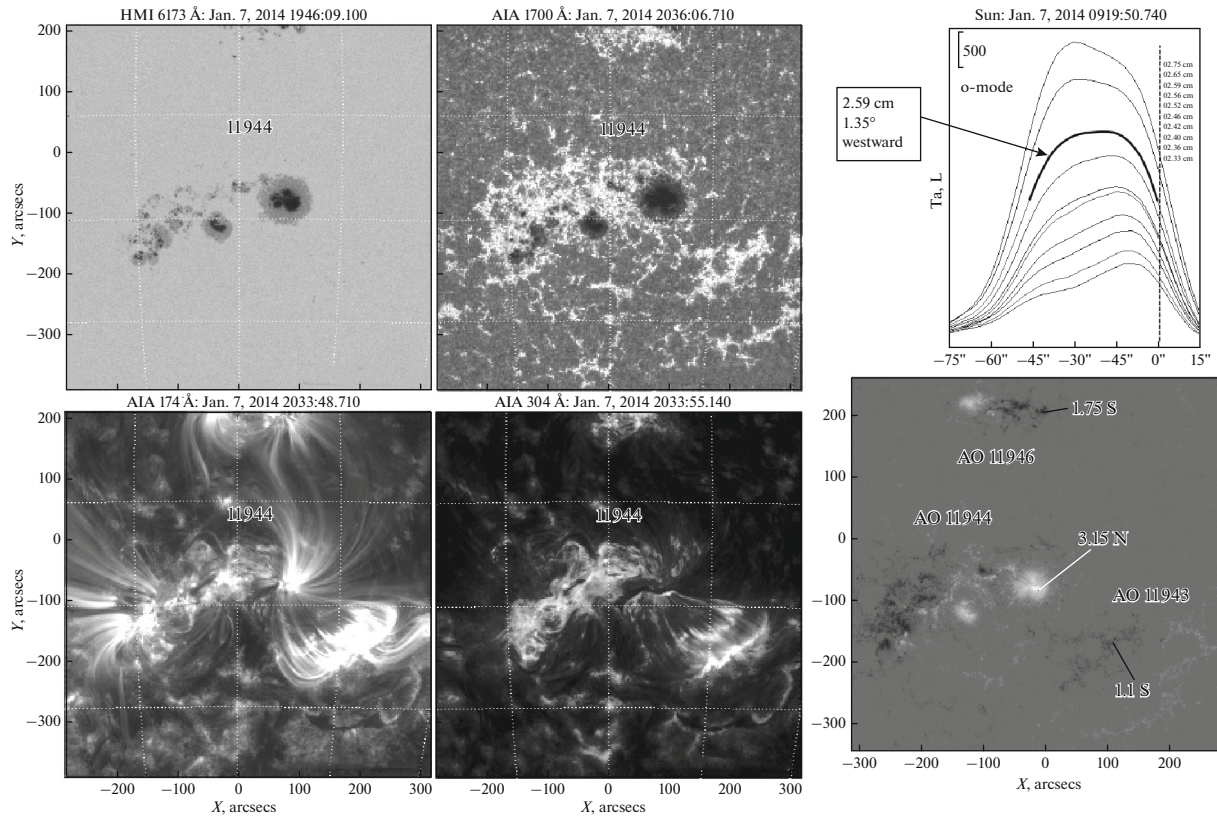


**Fig. 6.** Images of AR 11944 in UV lines 6173 Å (upper photosphere), 1700 Å (photospheric temperature minimum), 174 Å (upper transition region), and 304 Å (upper chromosphere). To the right of them are RATAN scans of AR 11944 and the magnetogram of a complex of ARs 11942 + 11943 + 11944 with indication of the sign (N/S) and MF value (in kG).

sufficient to use the standard processing, which makes it possible to “see” the tilt of the MF axis with the naked eye. However, the observations must occur regularly. This makes it possible to trace the CMRS image dynamics over a period of  $\pm(2-3)$  days within the PCM time. Due to the geographical distance of the observatories ( $\sim 94^\circ$  longitudinally), the NoRH and RATAN-600 instruments cover almost 0.5 light days and provide a good opportunity to implement our proposed method for the measurement of the sunspot MFTA.

#### 4. CONCLUSIONS

1. A new method was proposed for the tilt-angle measurement of the sunspot magnetic field axis. It is based on the theory and on observations of solar microwave radiation. In contrast to the methods developed in the optical band that are used to measure the MF at the photospheric level, the radio method makes it possible to measure the tilt of the MF axis of sunspots above this level, i.e., already in the Sun’s atmosphere throughout the chromosphere–corona transition region from 2000 km to heights of  $\sim 10000$  km.

2. The proposed method was tested with solar observations by the world’s largest instruments, the RATAN-600 radio telescope and the NoRH. It was

shown that the characteristic tilt angles of the MF of the leading sunspots are small and are within  $1^\circ-10^\circ$  and that the axis is mainly directed toward the east, which agrees with the morphology of a typical bipolar AR (the MF of the leading sunspot is closed on tail sunspots).

3. Once again (following Hildebrandt et al., 1984), it was stated that the geometrical effects **must be considered** during the interpretation of the observations and the determination of the physical parameters of coronal plasma in order to avoid unjustified conclusions.

4. It was noted that the proposed method does not require any special processing of observations (beyond standard processing). However, its implementation requires high quality observations, preferably with the highest achievable angular, spectral, and temporal resolution.

#### ACKNOWLEDGMENTS

We thank the RATAN-600 and NoRH teams, who ensure the operation of these instruments and make their data freely available.

## FUNDING

This work was supported by the government contract of the Special Astrophysical Observatory of the Russian Academy of Sciences and approved by the Ministry of Science and Higher Education of the Russian Federation.

## CONFLICT OF INTEREST

The authors declare that they have no conflict of interest.

## REFERENCES

- Bakunina, I.A., Smolkov, G.Ya., and Snegirev, S.D., On “geometric” effects in the microwave radiation of active regions passing through the solar disk, *Radiophys. Quantum Electron.*, 2008, vol. 51, no. 8, pp. 579–596. <https://doi.org/10.1007/s11141-008-9064-0>
- Bogod, V.M. and Yasnov, L.V., Vertical structure of the magnetic field in active regions of the Sun at coronal heights, *Cosmic Res.*, 2008, vol. 46, no. 4, pp. 309–313. <https://doi.org/10.1134/S0010952508040047>
- Bogod, V.M. and Yasnov, L.V., Determination of the structure of the coronal magnetic field using microwave polarization measurements, *Sol. Phys.*, 2016, vol. 291, no. 11, pp. 3317–3328. <https://doi.org/10.1007/s11207-016-0936-8>
- Gopasyuk, O.S., Magnetic field of sunspots during the rising phase of activity cycle 24, *Astrophysics*, 2017, vol. 60, no. 1, pp. 90–99. <https://doi.org/10.1007/s10511-017-9465-x>
- Gopasyuk, O.S., The magnetic field structure of a single spot, *Kinematika Fiz. Nebesnykh Tel*, 2003, vol. 19, no. 2, no. 1, pp. 126–137.
- Hildebrandt, J., Seehafer, N., and Kruger, A., An example of a solar S-component model calculation using force-free magnetic field extrapolation, *Astron. Astrophys.*, 1984, vol. 134, no. 1, pp. 185–188.
- Maunder, A.S.D., An apparent influence of the Earth on the numbers and areas of sun-spots in the cycle 1889–1901, *Mon. Not. R. Astron. Soc.*, 1907, vol. 67, pp. 451–476.
- Topchilo, N.A. and Peterova, N.G., On inclination of the magnetic field of sunspots according to microwave observations, in *Tr. XXII Vseross. konf. po fizike Solntsa “Solnechnaya i solnechno-zemnaya fizika-2018”* (Proc. XXII All-Russian Conf. on Solar Physics “Solar and Solar–Terrestrial Physics”), St. Petersburg, GAO RAS, 2018, pp. 373–376. <https://doi.org/10.31725/0552-5829-2018-373-376>
- Topchilo, N.A. and Peterova, N.G., Measurement of inclination angle of the magnetic field of sunspots (method and results), *Tr. XXIII Vseross. konf. po fizike Solntsa “Solnechnaya i solnechno-zemnaya fizika-2019”* (Proc. XXIII All-Russian Conf. on Solar Physics “Solar and Solar–Terrestrial Physics”), St. Petersburg, GAO RAS, 2019, pp. 407–410. <https://doi.org/10.31725/0552-5829-2019-407-410>
- Vourlidas, A., Gary, D.E., and Shibasaki, K., Sunspot gyroresonance emission at 17 GHz: A statistical study, *Publ. Astron. Soc. Jpn.*, 2006, vol. 58, no. 1, pp. 11–20. <https://doi.org/10.1093/pasj/58.1.11>
- Zagainova, Yu.S., Fainshtein, V.G., Obridko, V.N., and Rudenko, V.G., Comparison of magnetic properties and shadow area of leading and trailing spots with different asymmetries, *Geomagn. Aeron. (Engl. Transl.)*, 2017, vol. 57, no. 8, pp. 946–951. <https://doi.org/10.1134/S0016793217080266>
- Zlotnik, E.Ya., Theory of the slowly changing component of solar radio emission. I., *Sov. Astron.*, 1968a, vol. 12, no. 2, pp. 245–253.
- Zlotnik, E.Ya., The theory of the slowly changing component of solar radio emission. II., *Sov. Astron.*, 1968b, vol. 12, no. 3, pp. 464–472.

*Translated by O. Pismenov*